



# Journal of Applied and Computational Mechanics



Research Paper

## Numerical Analysis of Resource Characteristics of Structural Elements under Thermocycling Loading

Leonid Igumnov<sup>1</sup>, Ivan Volkov<sup>1</sup>, Andrey Volkov<sup>1</sup>, Victor A. Eremeyev<sup>2,3</sup>

<sup>1</sup> National Research Lobachevsky State University of Nizhny Novgorod, 23 Gagarin Avenue, building 6, Nizhny Novgorod 603950, Russian Federation

<sup>2</sup> Department of Mechanics of Materials and Structures, Faculty of Civil and Environmental Engineering, Gdansk University of Technology, 11/12 Gabriela Narutowicza Street, Gdansk, 80-233, Poland

<sup>3</sup> Department of Civil and Environmental Engineering and Architecture (DICAAR), University of Cagliari, Via Marengo, 2, 09123 Cagliari, Italy

Received March 08 2024; Revised May 05 2024; Accepted for publication May 27 2024.

Corresponding author: V.A. Eremeyev (eremeyev.victor@gmail.com)

© 2024 Published by Shahid Chamran University of Ahvaz

**Abstract.** We discuss methodological aspects of assessment of the service life of structures and devices used in new technologies, paying a particular attention to non-stationary thermomechanical loading of “dangerous” zones of the systems under investigation. As result, using the approach of modern mechanics of the degradable continuum, we develop a model describing the associated processes of viscoplastic deformation and damage accumulation and adapted it to description of thermal fatigue. The presented model describes the main effects of inelastic deformation and damage accumulation processes in polycrystalline structural alloys for arbitrary complex deformation trajectories. A combined form of the kinetic equations for damage accumulation in the areas of interaction between low-cycle fatigue and long-term strength has been proposed, which makes it possible to properly describe the nonlinear nature of the damage accumulation.

**Keywords:** Thermocyclic durability, continuum damage mechanics, viscoplasticity, complex deformations, fracture.

### 1. Introduction

The operation of critical infrastructure facilities is characterized by a significant increase in the proportion of non-stationary loading modes and an extension of the temperature range of operation of structures. Requirements for safety, reliability and long-term operations are becoming more stringent. One of the main tasks of effective management of such an object is the reliable calculation of the resource, diagnostics of the exhausted resource and forecast of the remaining resources [1, 2]. From the relevant engineering facilities, we mention those ones that are oriented towards long service life, such as oil and gas equipment, new generation gas turbine engines and installations (GTE), nuclear power plants (NPP), etc. The solution to the main problems of determining the resource is based on taking into account the local manifestation of degradation processes in the “dangerous” zones of the object, passing at an increased speed, which makes it possible to calculate the service life of structural elements. At the same time, the parameters of degradation processes vary essentially depending on the physical, mechanical and strength properties of structural alloys, characteristic manufacturing features and a number of other factors.

The methodology for operational resource monitoring was proposed in [2]. The approach is based on the method of mathematical modeling within the framework of the continuum damage mechanics (CDM) and fracture mechanics (FM). The approach makes it possible to take into account abnormal operating conditions of the object, real physical and mechanical characteristics of the material, and a number of beyond design conditions. Non-destructive testing methods are used to check the condition of the material in “dangerous” zones.

Under thermomechanical conditions, their characteristic degradation mechanisms are revealed, leading to a decrease in fatigue life. The rate of change in load (mechanical deformation) and temperature, and the duration of a loading cycle are significant. When assessing durability, the total number of cycles to failure becomes an incomplete characteristic of durability, and time to failure must be taken into account [3-6]. The difference in failure mechanisms is the result of different damage processes, in general. One of these processes occurs under the dominant influence of plastic deformation, which depends only on changes in the load without taking into account its duration. Such damage accumulates inside alloy grains and leads to a transgranular fracture. Damage from unsteady creep deformation depends on the loading history, the duration of the load, and leads to the development of damage along the grain boundaries. As a result, intracrystalline destruction occurs.

Synergistic effects of the mutual influence of damage mechanisms occur in the intermediate region, where both types of destruction processes occur simultaneously. Durability in this area is determined by the summation of damage caused by both processes [7, 8]. In [7-10], a variant of the damaged medium model was proposed for the associated processes of non-isothermal viscoplastic deformation and damage accumulation under multiaxial disproportionate modes of cyclic thermomechanical loading.

In this paper, based on a general approach and a model for a coupled thermomechanical formulation, we present the analysis of the resource of flame tubes of combustion chambers under thermal pulsations, that used in modern gas turbine engines.



## 2. Basic Relations of the Model of Continuum Damage Mechanics

The basic equations of the model proposed in [7, 8] and developed in [9, 10] are the constitutive relations of thermoviscoplasticity: thermoplasticity [11], thermocreep [12], evolution equations of damage accumulation and the strength criterion of damaged material [8], listed below:

a) Thermoviscoplasticity

- Mises flow equation:

$$S_{ij}S_{ij} - C_p^2 = 0, \quad S_{ij} = \sigma'_{ij} - \rho_{ij}^p, \quad (1)$$

where  $\sigma'_{ij}$  are the components of the stress deviator,  $C_p$  and  $\rho_{ij}^p$  are the radius and coordinates of the center of the yield surface, respectively.

- Equation of the surface of cyclic "memory":

$$a_e = (e_{ij}^p - \xi_{ij})(e_{ij}^p - \xi_{ij}) - c_{\max}^2 = 0, \quad (2)$$

where  $e_{ij}^p$  are the components of the plastic deformation tensors,  $c_{\max}$  and  $\xi_{ij}$  are the maximum value of the intensity of plastic deformations and one-sided accumulated plastic deformations, respectively.

- Evolution equation for the radius of the yield surface:

$$C_p = C_p^0 + \int_0^t \dot{C}_p dt, \quad \dot{C}_p(\chi, T) = \dot{C}_p^{\text{mon}} + \dot{C}_p^{\text{p(cyc)}} + \dot{C}_p^T, \quad (3)$$

$$\dot{C}_p^{\text{mon}}(\chi, T) = q_\chi \dot{\chi}_p^{\text{mon}}, \quad \dot{C}_p^{\text{p(cyc)}} = a_p(Q_p^p - C_p^{\text{p(cyc)}}) \dot{\chi}_p^{\text{cyc}},$$

$$\dot{C}_p^{\text{c(cyc)}} = a_p(Q_p^c - C_p^{\text{c(cyc)}}) \dot{\chi}_c^{\text{cyc}}, \quad \dot{C}_p^T = q_T \dot{T}, \quad (4)$$

$$q_\chi = q_2 A + (1 - A) q_1, \quad Q_p^p = Q_2^p A + (1 - A) Q_1^p, \quad Q_p^c = Q_2^c A + (1 - A) Q_1^c,$$

$$A = 1 - \cos^2 \Theta, \quad \cos \Theta = n_{ij}^e n_{ij}^s, \quad n_{ij}^e = \frac{\dot{e}'_{ij}}{(\dot{e}'_{ij} \dot{e}'_{ij})^{1/2}}, \quad n_{ij}^s = \frac{S_{ij}}{(S_{ij} S_{ij})^{1/2}}, \quad (5)$$

$$\chi_p = \int_0^t \dot{\chi}_p dt, \quad \dot{\chi}_p = \left( \frac{2}{3} \dot{e}_{ij}^p \dot{e}_{ij}^p \right)^{1/2}, \quad \dot{\chi}_p^{\text{cyc}} = \begin{cases} \dot{\chi}_p, & a_e < 0 \vee e_{ij}^p \dot{e}_{ij}^p \leq 0, \\ 0, & a_e = 0 \wedge e_{ij}^p \dot{e}_{ij}^p \geq 0, \end{cases} \quad (6)$$

$$\dot{\chi}_p^{\text{mon}} = \begin{cases} 0, & a_e < 0 \vee e_{ij}^p \dot{e}_{ij}^p \leq 0, \\ \dot{\chi}_p, & a_e = 0 \wedge e_{ij}^p \dot{e}_{ij}^p \geq 0, \end{cases}$$

where  $C_p^0$  is the value of the initial radius of the yield surface;  $q_1, q_2, q_T$  - parameters of monotonic isotropic hardening;  $Q_1^p, Q_2^p, Q_1^c, Q_2^c$  are the parameters of cyclic isotropic hardening;  $\chi_p$  is the length of the path of plastic deformation,  $\dot{\chi}_p^{\text{mon}}, \dot{\chi}_p^{\text{cyc}}, \dot{\chi}_c^{\text{cyc}}$  and is the length of the path of plastic deformation in monotonic sections, in sections of cyclic loading and in sections of holding under load, respectively.

- Equation for the displacement of the center of the yield surface:

$$\rho_{ij} = \int_0^t \dot{\rho}_{ij} dt, \quad \dot{\rho}_{ij} = \dot{\rho}_{ij}^p + \dot{\rho}_{ij}^c, \quad \dot{\rho}_{ij}^p = f(\chi)(\dot{\rho}_{ij}^m + \dot{\rho}_{ij}^r), \quad \dot{\chi} = \dot{\chi}_p + \dot{\chi}_c, \quad (7)$$

$$\dot{\rho}_{ij}^m = g_1^p \dot{e}_{ij}^p - g_2^p \rho_{ij}^p \dot{\chi} + g_7^p \rho_{ij}^p \langle \dot{T} \rangle, \quad \dot{\rho}_{ij}^r = g_1^r \dot{e}_{ij}^p - g_2^r \left( \frac{\rho_{\min}^r - \rho_u^r}{\rho_u^r} \right) \rho_{ij}^r \dot{\chi} \cos \gamma + g_7^r \rho_{ij}^r \langle \dot{T} \rangle, \quad (8)$$

$$\cos \gamma = \begin{cases} \frac{\dot{\rho}_{ij}^r \rho_{ij}^r}{(\dot{\rho}_{ij}^r \dot{\rho}_{ij}^r)^{1/2} (\rho_{ij}^r \rho_{ij}^r)^{1/2}}, & \cos \gamma < 0, \\ 0, & \cos \gamma > 0, \end{cases} \quad \rho_u^r = (\rho_u^r \rho_u^r)^{1/2}, \quad g_{7,r}^{p,r} = \frac{1}{g_{1,r}^{p,r}} \left[ \frac{\partial g_{1,r}^{p,r}}{\partial T} \right], \quad (9)$$

$$f(\chi) = f(\chi_p^{\text{mon}}) + f(\chi_p^{\text{cyc}}) + f(\chi_c) + f(\chi_\xi), \quad (10)$$

$$f(\chi_{c,\xi}) = 1 + k_1^{\xi,c} (1 - \exp(-k_2^{\xi,c} \chi_{c,\xi})),$$

where  $g_{1,r}^{p,r}, g_{2,r}^{p,r}, k_1^{\xi,c}, k_2^{\xi,c}$  are the material parameters.

Hereinafter, the following definition are used for  $\dot{T}$ :

$$\langle \dot{T} \rangle = \begin{cases} \dot{T}, & \dot{T} > 0, \\ 0, & \dot{T} \leq 0. \end{cases}$$

- Equations of the family of equipotential creep surfaces:

$$F_e^{(n)} = S_{ij}^{(n)} S_{ij}^{(n)} - C_c^{2(n)} = 0, \quad S_{ij}^{(n)} = \sigma'_{ij} - \rho_{ij}, \quad n = 0, 1, 2, \dots, \quad (11)$$



- Equation of the zero-level creep surface:

$$F_c^{(0)} = \bar{S}_{ij}^c \bar{S}_{ij}^c - \bar{C}_c^2 = 0, \quad \bar{S}_{ij}^c = \bar{\sigma}_{ij}^c - \rho_{ij}. \quad (12)$$

where  $\bar{S}_{ij}^c$  and  $\bar{\sigma}_{ij}^c$  are the set of stress states corresponding to zero creep rate;

- Ratio for the radius of the creep surface of zero level:

$$\bar{C}_c = \bar{C}_c^{mon}(\chi_c^{mon}, T) + \bar{C}_c^{cyc}(\chi_c^{cyc}, T),$$

$$\bar{C}_c^{cyc} = \bar{C}_c^{0cyc} + \int_0^t \dot{\bar{C}}_c^{cyc} dt, \quad \dot{\bar{C}}_c^{cyc} = a_c(Q_c^p - C_c^{cyc})\dot{\chi}_c^{cyc}, \quad Q_c^p = Q_2^c A + (1-A)Q_1^c,$$

$$\dot{\chi}_c = \left( \frac{2}{3} \dot{e}_{ij}^c \dot{e}_{ij}^c \right)^{1/2}, \quad \chi_c = \int_0^t \dot{\chi}_c dt, \quad (13)$$

$$\dot{\chi}_c^{mon} = \begin{cases} 0, & a_e < 0 \vee e_{ij}^c \dot{e}_{ij}^c \leq 0, \\ \dot{\chi}_c, & a_e = 0 \wedge e_{ij}^c \dot{e}_{ij}^c \geq 0, \end{cases} \quad \dot{\chi}_c^{cyc} = \begin{cases} \dot{\chi}_c, & a_e < 0 \vee e_{ij}^c \dot{e}_{ij}^c \leq 0, \\ 0, & a_e = 0 \wedge e_{ij}^c \dot{e}_{ij}^c \geq 0, \end{cases}$$

$$\lambda_c = \lambda_c(\psi_c, T) = \lambda_c \psi_c,$$

where  $\bar{C}_c^{mon}$  and  $\lambda_c$  are some experimental functions.

- Equation for the displacement of coordinates of the center of creep surfaces [12]:

$$\dot{\rho}_{ij}^c = g_1^c \dot{e}_{ij}^c - g_2^c \rho_{ij}^c \dot{\chi}_c + g_3^c \rho_{ij}^c \langle \dot{T} \rangle,$$

where  $g_1^c$  and  $g_2^c > 0$  are again the material parameters.

- Normal rule:

$$\dot{e}_{ij}^c = \lambda_c(\psi_c, T) S_{ij}^c = \lambda_c \psi_c S_{ij}^c = \lambda_c \left( \frac{\sqrt{S_{ij}^c S_{ij}^c} - \bar{C}_c}{C_c} \right) S_{ij}^c,$$

whence

$$\dot{\chi}_c = \sqrt{\frac{2}{3}} \lambda_c \left( \sqrt{S_{ij}^c S_{ij}^c} - \bar{C}_c \right).$$

where from  $\lambda_c = \frac{\dot{\chi}_c}{\sqrt{2/3}(\sqrt{S_{ij}^c S_{ij}^c} - \bar{C}_c)}$ . The value of parameter  $\lambda_c$  depends on the section of the creep curve (see Fig. 1).

For the range  $(0 - \chi_c^{(1)})$ :

$$\lambda_c^I = \lambda_c^{(0)} \left( 1 - \frac{e_{11}^c}{e_{11}^{c(1)}} \right) + \lambda_c^{(1)} \frac{e_{11}^c}{e_{11}^{c(1)}}, \quad (14)$$

where  $\lambda_c^{(0)}$  and  $\lambda_c^{(1)}$  is the value at points "0" and "1".

For the range  $(\chi_c^{(1)} - \chi_c^{(2)})$ :

$$\lambda_c^{II} = \frac{3}{2} \frac{\dot{e}_{11}^{e(est)}}{(\sigma_{11}' - (3/2)\rho_{11}^c - \bar{\sigma}_c)}. \quad (15)$$

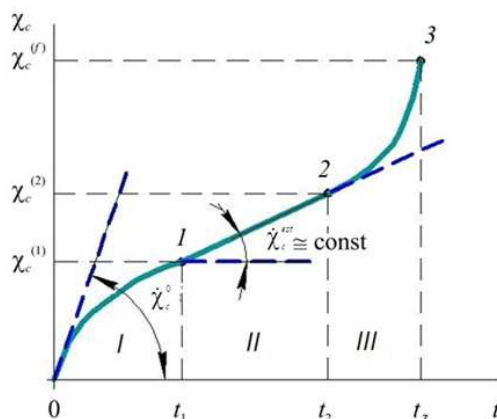


Fig. 1. Dependence of the length of the creep deformation trajectory on the process time during multiaxial deformation along ray trajectories.



For the range ( $\chi_c > \chi_c^{(2)}$ ):

$$\lambda_c^{III} = \frac{\lambda_c^{II}}{1 - \omega}, \quad (16)$$

where  $\omega$  is the material damage parameter.

The algorithm for connecting the thermoplasticity equations (1) to (10) with the thermocreep equations (11) to (16) is that stresses, creep plasticity strains are found from the thermocreep equations by the Runge-Kutta method. The stress deviator is corrected by determining the stresses from the thermoplasticity equations at the average creep strain rate at every new time interval.

#### b) Accumulation of damage

The process of damage accumulation is given in the form [13-16]:

$$\dot{\omega} = f_1(\beta) f_2(\omega) f_3(W_0) f_4(\Theta) \dot{W}_0, \quad W_0 = \rho_{ij} \dot{e}_{ij}^n, \quad \dot{e}_{ij}^n = \dot{e}_{ij}^p + \dot{e}_{ij}^c \quad (17)$$

where  $f_i, i = \overline{1, 4}$ , are the following functions:  $f_1(\beta)$  is the "volume" of the stress state;  $f_2(\omega)$  is the level of accumulated damage;  $f_3(W_0)$  is the value of the relative "dangerous" energy  $W_0$  used for the formation of microdefects;  $f_4(\Theta)$  is a function that takes into account the influence of the parameters of the deformation trajectory defined as follows:

$$f_1(\beta) = \exp k\beta, \quad (18)$$

$$f_2(\omega) = \begin{cases} 0, & W_0 \leq W_a, \\ \omega^{1/3} (1 - \omega)^{2/3} & W_0 > W_a \wedge \omega \leq 1/3, \\ \sqrt[3]{16/9} \omega^{-1/3} (1 - \omega)^{-2/3} & W_0 > W_a \wedge \omega > 1/3, \end{cases} \quad (19)$$

$$f_3(W_0) = \frac{W_0 - W_a}{W_f - W_a}, \quad W_f = W_{pf}^{cyc} \frac{\dot{\chi}_p^{cyc}}{\dot{\chi}} + W_{cf}^{cyc} \frac{\dot{\chi}_c^{cyc}}{\dot{\chi}} + W_{pf}^{mon} \frac{\dot{\chi}_p^{mon}}{\dot{\chi}} + W_{cf}^{cyc} \frac{\dot{\chi}_c^{mon}}{\dot{\chi}}, \quad (20)$$

$$W_f = W_{pf}^{cyc} \frac{\dot{\chi}_p^{cyc}}{\dot{\chi}} + W_{cf}^{cyc} \frac{\dot{\chi}_c^{cyc}}{\dot{\chi}} + W_{pf}^{mon} \frac{\dot{\chi}_p^{mon}}{\dot{\chi}} + W_{cf}^{cyc} \frac{\dot{\chi}_c^{mon}}{\dot{\chi}},$$

$$f_4(\Theta) = (1 - \cos^2 \theta) \beta + \cos^2 \theta. \quad (21)$$

where  $W_a, W_a, W_{pf}^{cyc, mon}(T)$  and  $W_{cf}^{cyc, mon}(T)$  are the material parameters dependent on temperature.

#### c) Strength

For the damage criterion we choose the condition [8]:

$$\omega = \omega_f \leq 1. \quad (22)$$

The model of the damaged medium (its components a-c) are "coupled" by introducing effective stresses [7, 8]:

$$\bar{\sigma}'_{ij} = F_1(\omega) \sigma'_{ij} = \frac{G}{G} \sigma'_{ij} = \frac{\sigma'_{ij}}{(1 - \omega)[1 - (6K + 12G) / (9K + 8G)\omega]} \quad (23)$$

$$\bar{\sigma} = F_2(\omega) \sigma = \frac{K}{K} \sigma = \frac{\sigma}{4G(1 - \omega) / (4G + 3K\omega)}, \quad \bar{\rho}_{ij} = F_1(\omega) \rho_{ij}, \quad (24)$$

where  $\bar{G}, \bar{K}$  are the effective elastic moduli, determined by the Mackenzie formulas [17].

Thus, modeling of these processes leads to the need to integrate nonlinear ordinary differential equations with initial conditions. The choice of an effective algorithm for the numerical integration of these equations is of decisive importance for ensuring the stability of the process of calculating the parameters of the deformation process and reducing the calculation time.

Determination of the main characteristics of the process of viscoplastic deformation of damaged materials (state parameters), which in the general case are described by tensors  $\sigma'_{ij}, e_{ij}, e_{ij}^p, \rho_{ij}^p, e_{ij}^c$  and scalars  $\chi, C_p, C_c, T$  and  $\omega$  can be carried out with the appropriate formulation of the constitutive relations of the CDM in increments that depend on the selected step  $\Delta t$ . The time step  $\Delta t$  can be adjusted when passing through complex sections of the deformation trajectory throughout the entire calculated time, provided that the calculations are stable (explicit Euler scheme).

This approach is most convenient for solving boundary value problems in the mechanics of a deformable solid and is used in this work.

With the mutual influence of the processes of plasticity and creep, stresses, plastic deformations and creep deformations are determined by integrating the thermocreep equations (11) to (16) by the four-point Runge-Kutta method with correction of the stress deviator and subsequent determination of stresses according to the thermoplasticity equations (1) to (10) taking into account average creep strain rate at time:  $t_{n+1} = t_n + \Delta t$ .

### 3. Research Results

Trouble-free operation of gas turbine engines and installations is ensured by new heat-resistant materials, cooling systems and parts protection means [18-21]. With the help of such systems and means, it is possible to achieve an increase in thermal cycle durability by more than 5 times. Currently used heat-resistant alloys operate at maximum permissible temperatures.



**Table 1.** Chemical composition of the VZh-159.

Fe, %	Si, %	B, %	Mg, %	Mn, %	Co, %	Cr, %	Ti, %	Cu, %	Ni, %
< 3	< 0.8	< 0.005	< 0.03	< 0.5	< 0.2	26-28	< 0.2	< 0.07	53.879-63.01
V, %	Al, %	P, %	C, %	S, %	Nb, %	La, %	Y, %	Mo, %	W, %
< 0.2	1.25-1.55	< 0.013	0.04-0.08	< 0.013	2.7-3.4	< 0.03	< 0.03	7-7.8	< 0.2

**Table 2.** Thermocyclic durability.

Angle of inclination of the channel axis to the surface	Diameter, mm	Number of cycles to failure N							Average value Ncp
a) $\gamma = 35^\circ$	1	174	194	200	117	292	156	189	
b) $\gamma = 90^\circ$	1	851	950	983	576	1431	765	926	

In [20], the results of experimental and theoretical studies are presented on the influence of the angle of inclination of the cooling channels of models of flame tubes of combustion chambers on their thermal cyclic durability. Experimental data provide estimates of the influence of inclination angles and channel parameters on the thermal cyclic durability of models of flame tubes of combustion chambers of gas turbine engines.

Let us consider hollow box-shaped samples made of the VZh-159 heat-resistant alloy on a nickel base. A plug is installed at the upper end of the sample. The formation of a crack was observed through a binocular microscope, and a thermal imager of the temperature field of the perforated wall of the sample was used for control. Wall thickness 1 mm. Rows of holes with a diameter of 1; 1.5; 2 cm (Fig. 2a). On one side the holes are made perpendicular to the surface ( $\gamma = 90^\circ$ ), and on the other - at an angle  $\gamma = 35^\circ$  (Fig. 2b).

Thermocyclic trapezoidal heating is specified by increasing the temperature of the surface of the part by heating from 350°C to 900°C. The heating time was  $t = 5$  s. At the temperature 900°C, the hollow samples were kept for 7 s. Cooling air was supplied inside the sample at a constant flow rate 121 s.

Table 1 shows the chemical composition of the VZh-159 heat-resistant alloy on a nickel base (according to the standard GOST 5632-14) [22].

Table 2 shows the results of experiments with different angles of inclination of the cooling channels (hole diameter 1 mm).

Our studies show that the temperature gradient across the wall thickness of the sample with normal channels is lower and the temperature difference showed 250°C. The experimental results show a more than 5-fold decrease in the resource characteristics of pipe models with channels at angle 35°, compared to when angle 90°. In this case, the role of the size of the hole for supplying cooling air with design diameters is 1; 1.5; and 2 mm is insignificant (their effect on the thermal cycle life is no more than 20%).

The numerical solution is a sequential solution of the following problems: electromagnetic; thermal conductivity; calculation of service life characteristics under multiaxial stress conditions. From the solution of Maxwell's equation, the nonstationary distribution of specific heating power over the thickness of the pipe was found.

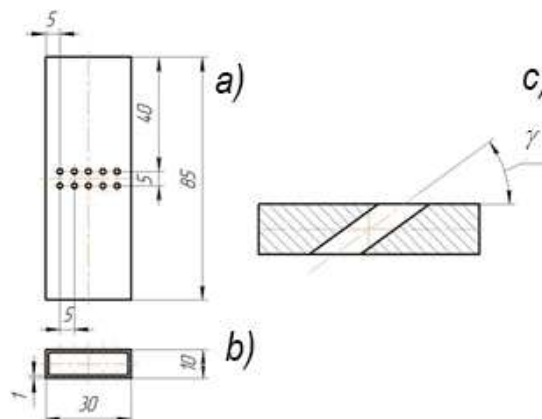
The calculation of the non-stationary thermal field for the cooled product was carried out using the ANSYS software package (Customer license 244793). In the calculations, the thermal conductivity and heat transfer of the environment were assumed to be 20° and 25 W/(m<sup>2</sup> K); heat transfer coefficient inside the pipe – 1900 W/(m<sup>2</sup> K); specific heating power –  $9 \times 10^5$  W/m<sup>2</sup>; range of product surface heating temperature from 350°C to 900°C. The solution was carried out in a coupled formulation.

Numerical analysis shows that the temperature gradient in the vicinity of normal channels is less than that near inclined ones. The temperature field is non-uniform and the temperature difference across the thickness for normal channels is 164.5°C (Fig. 3a), and for inclined channels - 264.3°C (Fig. 3b). The result is confirmed by experimental data.

The assessment of thermal cyclic durability at various angles was solved numerically using the found temperature fields [7-10].

The kinetics of stress-strain state in a nonlinear formulation was determined in the ANSYS software package. The distribution of the von Mises equivalent stress fields and the intensity of inelastic deformations of a fragment of a pipe model with perforated holes in the vicinity of one of the channels for the second cycle of thermocyclic stress is shown in Figs. 4 and 5 respectively. The highest von Mises equivalent stress is observed inside the pipe wall, while the maximum intensity of inelastic deformations occurs in the vicinity of the outer heated edge of the channel surface. It is noted [23] that it is in this area that degradation processes occur most intensively [20]. A microscopic crack has formed in this zone [20].

The study allows us to assert that thermal fatigue depends on the influence of the physical, mechanical and strength properties of the heat-resistant alloy on temperature and the process of "captivity" of the thin outer (heated) surface of the channel with the more rigid "cold" part of the wall.

**Fig. 2.** Laboratory sample scheme.

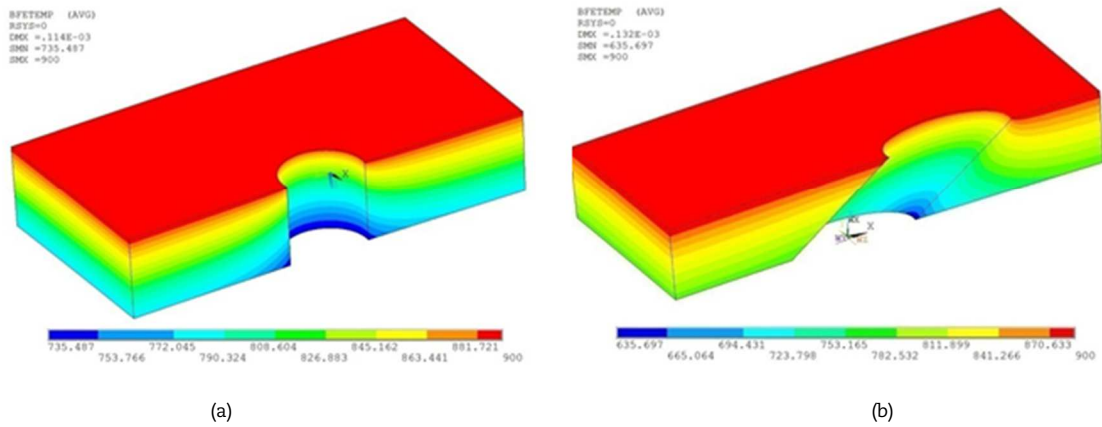


Fig. 3. Temperature fields °C in the vicinity of (a) normal channels, (b) inclined channels.

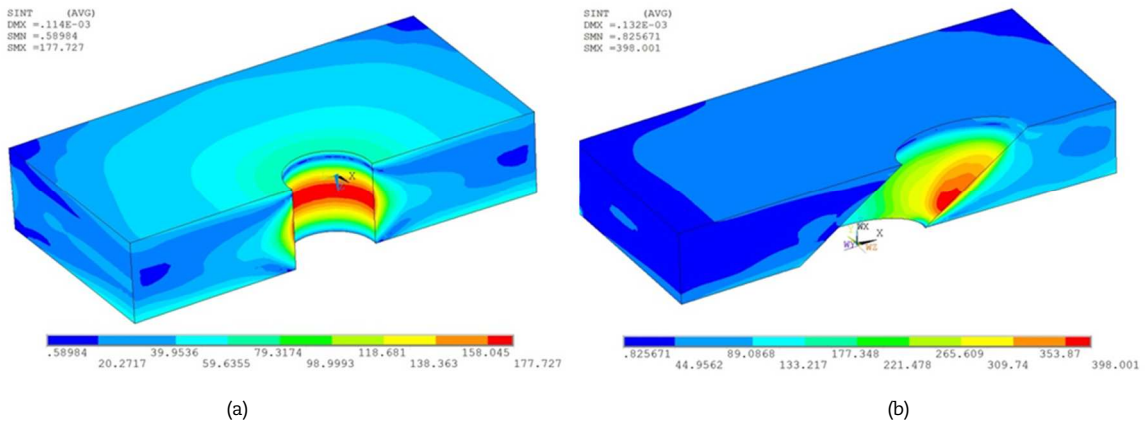


Fig. 4. Distribution of von Mises equivalent stress fields (MPa) of a fragment of a pipe model in the vicinity of one of the channels for the second cycle of thermocyclic stress.

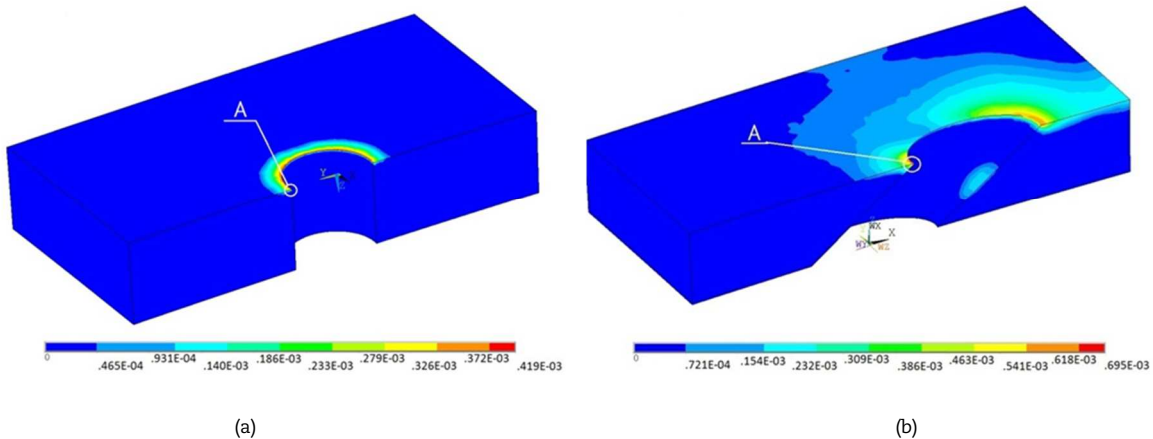


Fig. 5. Distribution of inelastic deformation intensity fields of a fragment of a pipe model in the vicinity of one of the channels for the second cycle of thermocyclic stress.

In the most loaded zone, we select point A. In the vicinity of point A (Fig. 5), a stress state close to a plane stress state is realized. At point A, the dependences of temperature and strain tensor components on the number of loading steps were obtained for two inclination angles of the cooling channels. These results were used to evaluate the thermal cycle life of the pipe using the EXPMODEL software tool. For point A in Figs. 6 and 7, the cyclic hysteresis loops are shown, calculated using the EXPMODEL software tool [8]:  $\sigma_{11} \sim \epsilon_{11}$  (Fig. 6),  $\sigma_{22} \sim \epsilon_{22}$  (Fig. 7). In Fig. 8, we present the loading trajectories ( $\sigma_{11} \sim \sigma_{22}$ ). The data obtained (Figs. 6 to 8) show the presence of rotation of the main areas of the stress and strain tensors, as well as the misalignment of the stress, total and inelastic strain tensors. In addition, it is clear that taking into account the formation of creep deformations (even minor ones) affects the shape of the cyclic hysteresis loop [23]. Integrating the evolutionary equation for the accumulation of fatigue damage makes it possible to show the effect of the angle of the cooling channels on the thermal cyclic durability (point A in Fig. 5). The dependence of damage values on the number of loading cycles is shown in Fig. 8. Experimental (Table) and calculated (Fig. 9) data show the necessary engineering accuracy of the results.



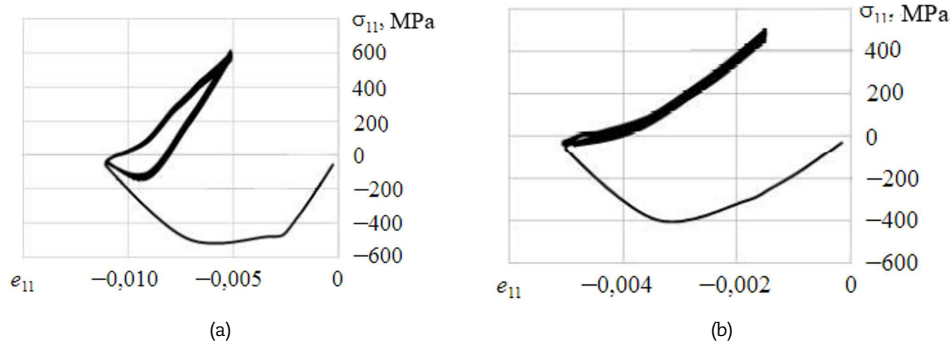


Fig. 6. Cyclic hysteresis loops calculated using the EXPMODEL software tool  $\sigma_{11} \sim e_{11}$  : (a)  $\gamma = 35^\circ$ , (b)  $\gamma = 90^\circ$ .

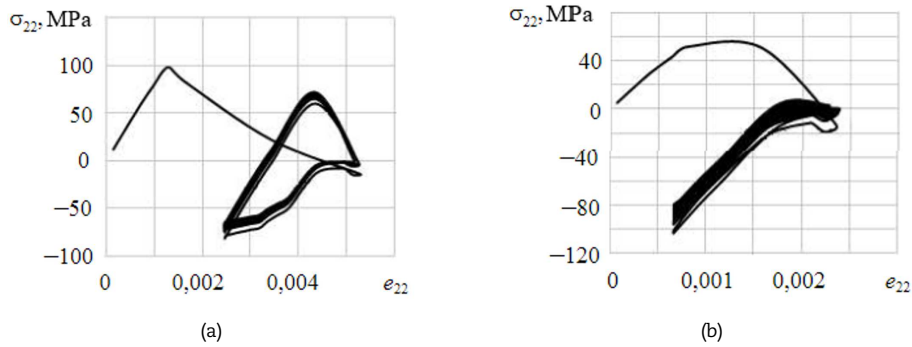


Fig. 7. Cyclic hysteresis loops calculated using the EXPMODEL software tool  $\sigma_{22} \sim e_{22}$  : (a)  $\gamma = 35^\circ$ , (b)  $\gamma = 90^\circ$ .

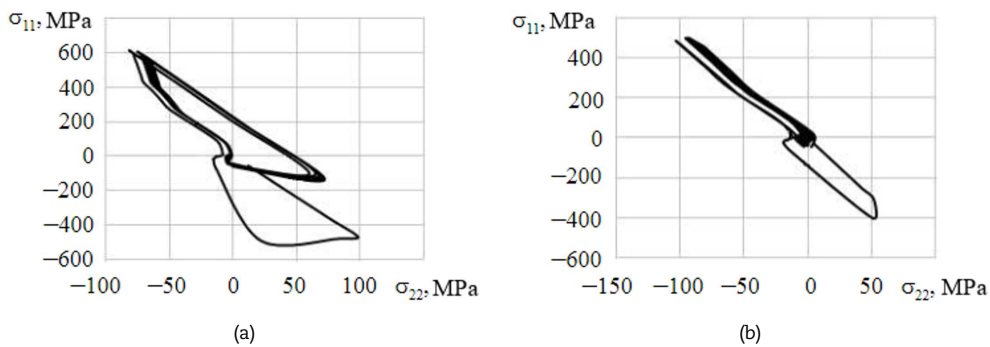


Fig. 8. Loading trajectories  $\sigma_{11} \sim \sigma_{22}$  : (a)  $\gamma = 35^\circ$ , (b)  $\gamma = 90^\circ$ .

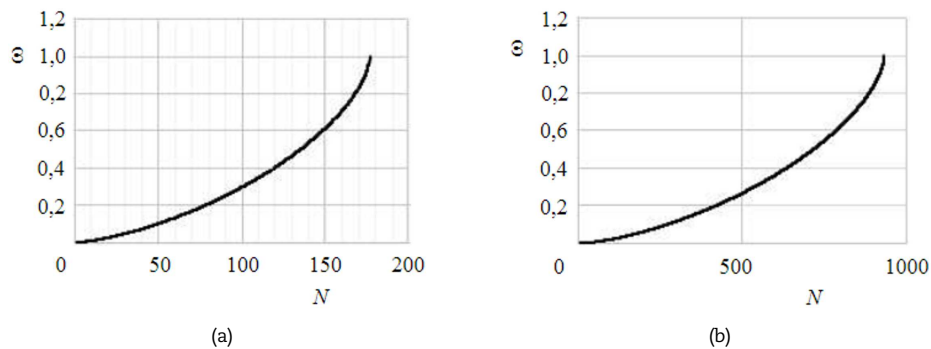


Fig. 9. Dependence of damage values on the number of loading cycles for two inclination angles of perforated holes: (a)  $\gamma = 35^\circ$ , (b)  $\gamma = 90^\circ$ .

Thus, using the developed EXPMODEL software and a methodology that provides end-to-end modeling (step-by-step calculation of the thermal state, a three-dimensional nonlinear problem of calculating the stress-strain state and further use of the obtained results as a condition for non-isothermal loading of the dangerous zone of the product), an assessment of the thermal cyclic durability of models of flame tubes of combustion chambers of modern gas turbine engines during thermal pulsations. The calculation results confirm the correctness of the approach to assessing the thermal cyclic durability of materials and structures and the adequacy of the developed model of the continuum damage mechanics.



## 4. Conclusion

An assessment of the reliability of the modified model of a continuum damage mechanics during material degradation by the mechanism of thermal fatigue was given. As an example, the calculation of models of flame tubes of combustion chambers of gas turbine engines was carried out. The design possibility of influencing resource characteristics has been demonstrated. Calculation showed that the decrease in thermal cyclic fatigue life is associated with a decrease in the angle of inclination of the perforated surfaces of the flame tubes of the combustion chambers, which is confirmed by experimental data. The research results confirmed the reliability of modeling the processes of complex thermocyclic deformation and assessing the thermal fatigue of materials and structures under multiaxial stress conditions.

## Author Contributions

L.A. Igumnov: the general management of research, setting tasks, participating in the discussion of results; I. Volkov: assistance in adapting the CDM model to solve problems of thermal cyclic fatigue durability of materials and structures; A. Volkov: assistance in carrying out calculations in the ANSYS software package; V.A. Eremeev: editing of the final text and participation in the discussion of the results. The manuscript was written through the contribution of all authors. All authors discussed the results, reviewed, and approved the final version of the manuscript.

## Acknowledgments

The authors would like to thank A.I. Yudintsev for preparing the article for publication.

## Conflict of Interest

The authors declared no potential conflicts of interest concerning the research, authorship, and publication of this article.

## Funding

The work was carried out with financial support from the State assignment of the Ministry of Education and Science of Russia (Project No. FSWR-2023-0036).

## Data Availability Statements

The datasets generated and/or analyzed during the current study are available from the corresponding author on reasonable request.

## References


- [1] Collins, J., *Failure of Materials in Mechanical Design: Analysis, Prediction, Prevention*, John Wiley & Sons, New York, 1981.
- [2] Mitenkov, F.M., Kaydalov, V.B., Korotkikh, Yu.G., et al., *Methods of Substantiating the Resource of Nuclear Power Plants*, Mashinostroenie Publ., Moscow, 2007.
- [3] Gomyuk, B.Q., Calculation durability stainless steel 304 in interaction of fatigue and creep by using the theory of continuous damage, *Transactions of the American Society of Mechanical Engineers, Series D*, 108(3), 1986, 111–136.
- [4] Zamrik, S.Y., Davis, D.C., A ductility exhaustion approach for axial fatigue – creep damage assessment using type 316 stainless steel, *ASME Journal of Pressure Vessel Technology*, 113(2), 1991, 180–186.
- [5] Zamrik, S.Y., An interpretation of axial creep-fatigue damage interaction in type 316 stainless steel, *ASME Journal of Pressure Vessel Technology*, 112(1), 1990, 4–19.
- [6] Zhang, T., Wang, X., Zhang, W., Hassan, T., Gong, J., Fatigue–Creep Interaction of P92 Steel and Modified Constitutive Modelling for Simulation of the Responses, *Metals*, 10(3), 2020, 307–318.
- [7] Volkov, I.A., Korotkikh, Yu.G., *Equations of State of Viscoelastic Plastic Media with Damage*, Fizmatlit Publ, Moscow, 2008.
- [8] Volkov, I.A., Igumnov, L.A., *Introduction to the Continuum Mechanics of a Damaged Medium*, Fizmatlit Publ, Moscow, 2017.
- [9] Igumnov, L.A., Volkov, I.A., Dellyizola, F., Litvinchuk, S.Yu., Eremeev, V.A., A continual model of a damaged medium used for analyzing fatigue life of polycrystalline structural alloys under thermal–mechanical loading, *Continuum Mechanics and Thermodynamics*, 32, 2020, 229–245.
- [10] Volkov, I.A., Igumnov, L.A., Shishulin, D.N., Boev, E.V., Modeling of non-stationary creep processes under multiple loading conditions by taking into account damage accumulation in a structural material, *Mechanics of Solids*, 57(2), 2022, 223–231.
- [11] Mitenkov, F.M., Volkov, I.A., Igumnov, L.A., et al., *Applied Theory of Plasticity*, Fizmatlit Publ, Moscow, 2015.
- [12] Volkov, I.A., Igumnov, L.A., Korotkikh, Yu.G., *Applied Theory of Viscoplasticity*, UNN Publ, Nizhny Novgorod, 2015.
- [13] Lemaitre, J., Chaboche, J., Aspect phenomenologique de la rupture par enclouement, *Journal de Mecanique Appliqué*, 2, 1978, 317–364.
- [14] Socie, D., Critical plane approaches for multiaxial fatigue damage assessment, *Advances in Multiaxial Fatigue*, ASTM STP 1191, 1993, 7–36.
- [15] Beaver, P.W., Biaxial Fatigue and Fracture of Metals, *Review Metals Forum*, 8, 1985, 14–29.
- [16] Chaboche, J.L., Continuous damage mechanics a tool to describe phenomena before crack initiation, *Engineering Design*, 64, 1981, 233–247.
- [17] MacKenzie, J.K., The elastic constants of a solids containing spherical holes, *Proceedings of the Physical Society*, B63, 1950, 2–11.
- [18] Bychkov, N.G., Lepeshkin, A.P., Pershin, A.V., Rekin, A.D., Lukash, V.P., Test procedure and evaluation of thermocyclic longevity of the models of the flame tubes of combustion chambers of GTE with protective coatings using high-frequency induction heating, *Aviation Engineering and Technology*, 8(16), 2004, 158–162.
- [19] Lepeshkin, A.R., Bychkov, N.G., Pershin, A.V., Thermo-physical measurements during thermal cycling of gas turbine engine blades with ceramic coatings, *High Temperature*, 48(5), 2010, 699–705.
- [20] Bychkov, N.G., Lepeshkin, A.P., Pershin, A.V., Reki, A.D., Lukash, V.P., Investigation of thermocyclic durability of parts with different angles of slope of cooled channels, *Aerospace Engineering and Technology*, 10(67), 2009, 113–117.
- [21] Igumnov, L.A., Volkov, I.A., Kazakov, D.A., Shishulin, D.N., Modin, I.A., Belov, A.A., Eremeyev, V.A., Experimental and theoretical study on high-temperature creep of VT6 titanium alloy under multi-axial loading conditions, *Journal of Thermal Stresses*, 2024, 1–16. <https://doi.org/10.1080/01495739.2024.2340602>
- [22] GOST 5632-14 Alloyed stainless steels and alloys, corrosion-resistant, heat-resistant and heat-resistant, introduced 2014-10-24, Moscow, 2015.
- [23] Volkov, I.A., Igumnov, L.A., Shishulin, D.N., Tarasov, I.S., Guseva, M.A., Numerical analysis of thermal-cyclic life of models of the flue tube with various inclinations of the cooling channels, *Problems of Strength and Plasticity*, 79(2), 2017, 220–233.


## ORCID iD

Leonid Igumnov  <https://orcid.org/0000-0003-3035-0119>





Ivan Volkov  <https://orcid.org/0000-0003-1176-4906>

Victor A. Eremeyev  <https://orcid.org/0000-0002-8128-3262>



© 2024 Shahid Chamran University of Ahvaz, Ahvaz, Iran. This article is an open access article distributed under the terms and conditions of the Creative Commons Attribution-NonCommercial 4.0 International (CC BY-NC 4.0 license) (<http://creativecommons.org/licenses/by-nc/4.0/>).

**How to cite this article:** Igumnov L., Volkov I., Volkov A., Eremeyev V.A. Numerical Analysis of Resource Characteristics of Structural Elements under Thermocycling Loading, *J. Appl. Comput. Mech.*, xx(x), 2024, 1–9.  
<https://doi.org/10.22055/JACM.2024.46323.4498>

**Publisher's Note** Shahid Chamran University of Ahvaz remains neutral with regard to jurisdictional claims in published maps and institutional affiliations.

